PHYSICAL REVIEW B

CONDENSED MATTER

THIRD SERIES, VOLUME 51, NUMBER 24 15 JUNE 1995-II

Near-infrared emission of Cr^{4+}-doped garnets: Lifetimes, quantum efficiencies, and emission cross sections

S. Kück,* K. Petermann, U. Pohlmann, and G. Huber

Institut für Laser-Physik, Universität Hamburg, Jungiusstraße 11, 20355 Hamburg, Germany

(Received 30 January 1995)

The lifetimes of the excited state of the tetrahedrally coordinated Cr^{4+} ion in several garnets were measured in the temperature range between 15 and 380 K. Both the nonradiative and radiative transition rates increase with temperature due to the coupling of phonons to the electronic states. This temperature dependence is described with the model of Struck and Fonger for the nonradiative decay rate and with the coth law for the radiative decay process. It is shown that even at low temperatures the nonradiative transition rate is larger than the radiative rate. With these data the quantum efficiencies are calculated to be between 8% and 33% at room temperature for the investigated crystals. The cross sections for the emission of the Cr^{4+} ion in the garnets are determined using the theory of McCumber. The $\sigma_{em}\tau$ product is highest for Cr^{4+}:$Lu_3Al_5O_{12}$, Cr^{4+}:$Y_3Al_5O_{12}$, and for Cr^{4+}:$Y_3Sc_xAl_{5-x}O_{12}$ crystals with low scandium content. Therefore, these crystals are most promising as tunable room-temperature lasers. A method for the calorimetric measurement of the quantum efficiency of the Cr^{4+} emission in yttrium aluminum garnet is also presented.

I. INTRODUCTION

The Cr^{4+} ion in tetrahedral coordination is interesting for the realization of tunable, room-temperature solid-state lasers in the near-infrared spectral range between 1.1 and 2 μm. The Cr^{4+} emission belongs to a transition between the $^3B_2(^3T_2)$ excited state into the $^3B_1(^3A_2)$ ground state, which is only magnetic-dipole allowed. $^3T_2$ and $^3A_2$ denote the energy levels in T_d symmetry (regular tetrahedron) and $^3B_2$ and $^3B_1$ denote the energy levels in D_{2d} symmetry (tetragonal distorted tetrahedron). The basic energy-level scheme is shown in Fig. 1. Until now, laser action at room temperature has been achieved with Cr^{4+}:Mg_2SiO_4,[1-3] Cr^{4+}:$Y_3Al_5O_{12}$,[4-5] Cr^{4+}:Y_2SiO_5,[6] and Cr^{4+}:$Y_3Sc_xAl_{5-x}O_{12}$.[7] The Cr^{4+} ion exhibits broadband emission because of the coupling between the electronic levels of the 3*d* electrons with the lattice vibrations. In addition, this electron-phonon coupling yields temperature-dependent nonradiative and radiative decay rates. The coupling phonons can be distinguished into two groups. The symmetric phonons do not influence the parity of the energy levels and increase the transition probability for the nonradiative decay only. The non-totally-symmetric phonons, on the other hand, induce parts of higher-energy levels of opposite parity to the transition and therefore raise also the radiative decay rate. Both result in a decrease of the lifetime of the upper laser level. In this paper, these temperature dependencies are discussed for different Cr^{4+}-doped garnet crystals on the basis of well-known models for the phonon coupling, i.e., the model of Struck and Fonger for the nonradiative rate,[8-10] and the coth law for the radiative decay process.[11-13] It is shown that the main difference in the lifetime of the excited state is caused by the difference in the energy gap between the excited state and the ground state

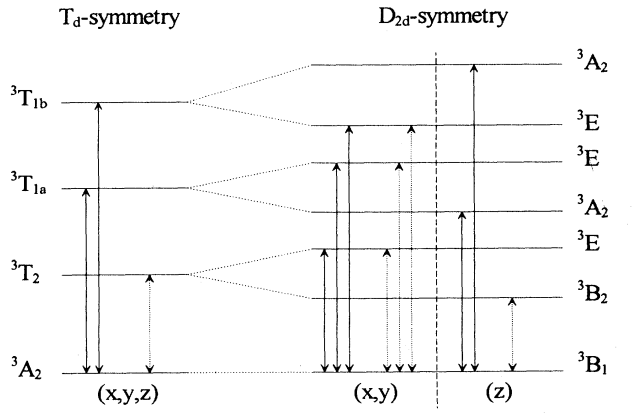

FIG. 1. Energy-level scheme of the tetrahedrally coordinated Cr^{4+} ion in T_d symmetry (regular tetrahedron) and D_{2d} symmetry (tetragonal distorted tetrahedron) with electric-dipole (——) and magnetic-dipole (— — —) allowed transitions. For clarity, only triplet levels are shown.

of the Cr^{4+} ion. With the measured data for the lifetimes and the calculated values for the quantum efficiency, the emission cross section and the $\sigma_{em}\tau$-product—both important parameters for the characterization of a laser material—are calculated. For Cr^{4+}:YAG, where YAG denotes yttrium aluminum garnet, the quantum efficiency was also directly measured.

II. EXPERIMENTAL

A. Crystal structure and crystal growth

Garnet crystals are cubic and belong to the space group $Ia3d$ (O_h^{10} in Schoenflies notation). The stoichiometric formula is $\{C_3\}[A_2](D_3)O_{12}$, where C, A, and D denote different lattice sites with respect to their oxygen coordination (dodecahedral, octahedral, and tetrahedral, respectively) and symmetry (222, $\bar{3}$, and $\bar{4}$, respectively). The optical active Cr^{4+} center occupies the tetrahedrally coordinated lattice site. Considering the nearest neighbors only, the crystal field at the place of the Cr^{4+} ion has D_{2d} symmetry. The crystals—listed in Table I—were grown by the Czochralski method using a high-frequency induction-heated iridium crucible. The chromium concentration was 0.05 at. % in the melt. Due to the trivalent tetrahedral site a divalent codoping of 0.01–0.9 at. % Ca or Mg as well as an oxidizing growth atmosphere is necessary in order to enhance the incorporation of tetravalent chromium. The growth rate was 3 mm/h, the rotation rate 20 rpm.

B. Spectroscopic measurements

For the fluorescence measurements the excitation light of a continuous wave Nd:YAG laser operating at 1064 nm was focused onto the crystal. The fluorescence was detected with a liquid-nitrogen cooled InSb detector, which was placed behind a 0.5 m monochromator. The fluorescence spectra were corrected for the response of the spectrometer-detector system. The lifetime measurements were carried out with a Q-switched Nd:YAG laser also operating at 1064 nm with a pulse width of 20 nsec. The excitation light was slightly focused onto the crystal. Here, the fluorescence was detected with a fast germanium diode, which was placed behind a 0.25 m monochromator. The fluorescence decay curve was measured with a storage oscilloscope; up to 400 decay curves were summed up in order to enhance the signal-to-noise ratio. For the emission and lifetime measurements between 77 and 380 K a nitrogen cryostat with temperature control was used, for temperatures below 77 K it was replaced by a helium cryostat.

For the calorimetric measurement of the quantum efficiency an argon-ion laser at 514.5 nm and a Nd:YAG laser at 1064 nm, both linear polarized, were used. The excitation beam of either the argon-ion laser or the Nd:YAG laser was slightly focused and aligned through a pinhole onto the Cr^{4+}:YAG crystal, which was adjusted under the Brewster angle to minimize the reflection. The pinhole was used to guarantee identical geometry for both excitation arrangements. The incident and the transmitted power were measured with a power meter. The crystal was placed onto a plastic block for thermal insulation and its temperature was measured with a thermocouple. The excitation time was 10 s in order to prevent the crystal from overheating.

III. RESULTS

A. Emission

The room-temperature emission spectra of several Cr^{4+}-doped garnet crystals under Nd:YAG-laser excitation are shown in Fig. 2. The emission band shifts to longer wavelengths with the increase of the lattice constant, as expected from the weakening of the crystal field. From these emission spectra the peak emission wavelengths and the bandwidths [full width at half maximum]

TABLE I. List of the investigated crystals with lattice constants, peak emission wavelengths, emission bandwidths, lifetimes, emission cross sections, and $\sigma_{em}\tau$-products at room temperature [* calculated with the formula of Strocka (Ref. 19); ** calculated with the formula of McCumber (Ref. 17); *** (Ref. 18)].

Lattice	Abbreviation	Lattice constant (Å)	λ_{max} (nm)	$\Delta\lambda$ (nm)	τ (300 K) (μs)	σ_{em}** (10^{-19} cm^2)	$\sigma_{em}\tau$ (10^{-24} s cm^2)
$Lu_3Al_5O_{12}$	LAG	11.91	1370	232	5.6	3.4	1.90
$Y_3Al_5O_{12}$	YAG	12.00	1378	224	4.1	3.3	1.35
$Y_3Sc_xAl_{5-x}O_{12}$	YSAG ($x=0.22$)	12.05*	1397	233	4.1	3.1	1.27
	YSAG ($x=0.48$)	12.09*	1407	237	3.3	3.3	1.09
	YSAG ($x=1.20$)	12.22*	1468	268	2.0	4.1	0.82
	YSAG ($x=1.50$)	12.27*	1508	303	1.5	4.5	0.68
	YSAG ($x=1.72$)	12.31*	1593	298	1.4		
$Y_3Ga_5O_{12}$	YGG	12.28	1456	238	1.9	4.3	0.82
$Gd_3Ga_5O_{12}$	GGG	12.38	1442	231	2.2	4.5	0.99
$Gd_3Sc_2Al_3O_{12}$	GSAG	12.39	1599	276	1.7	4.8	0.82
$Y_3Sc_2Ga_3O_{12}$	YSGG	12.42	1561	279	1.3	5.2	0.68
$Gd_3Sc_2Ga_3O_{12}$	GSGG	12.55	1582	299	2.0	3.6	0.72
Tl^{3+}:Al_2O_3***			760	250	3.1	4.5	1.40

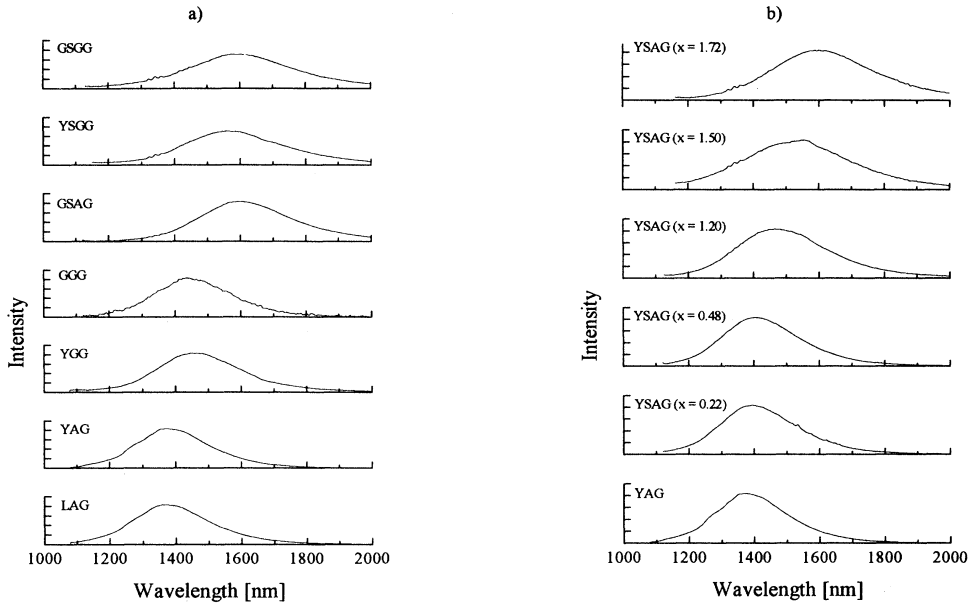

FIG. 2. Room-temperature emission spectra of Cr^{4+}-doped garnets.

are determined by fitting a Gaussian bandshape curve to the measured spectra. Because of the relative high value of the Huang-Rhys parameter ($S \approx 3$, see Sec. VI B), the approximation of a Gaussian bandshape instead of the Pekarian bandshape is valid. The results are listed in Table I.

B. Lifetimes

The lifetimes of the upper laser level of the Cr^{4+} ion in the temperature range between 15 and 380 K are shown in Fig. 3. The lifetime is a single exponential in the case of lutetium aluminum garnet (LAG), yttrium aluminum garnet (YAG), yttrium gallium garnet (YGG), and gadolinium gallium garnet (GGG) in the whole temperature range. For the scandium containing crystals they are not single exponential because of the statistical distribution of the scandium ions on the octahedral lattice site, which—in turn—results in different environments for the Cr^{4+} ions. Therefore in Fig. 3 the $1/e$ decay times are given. The lifetimes decrease with increasing temperature and also with increasing peak emission wavelength, as shown in Fig. 4.

IV. DISCUSSION

A. Quantum efficiency of the Cr^{4+} emission in YAG at room temperature

The quantum efficiency η is defined as the ratio of the radiative rate W_r and the total rate W of a transition. Under the assumption, that all absorbed photons lead to a relaxation into one metastable excited state, η can be expressed by the ratio of the number of emitted photons n_r and absorbed photons n_{abs}:

$$\eta = \frac{n_r}{n_{abs}} .$$

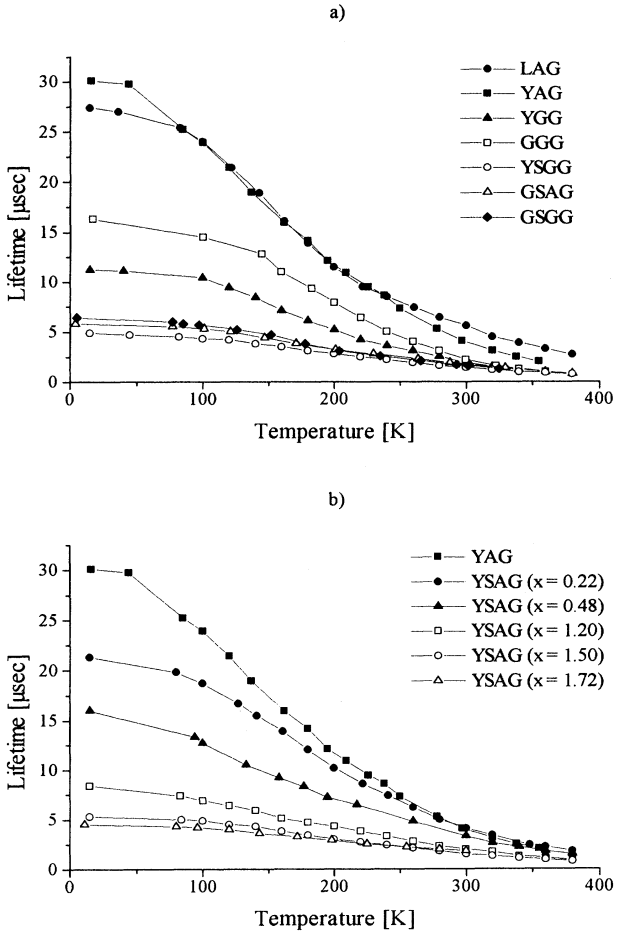

FIG. 3. Temperature dependence of the upper laser level lifetime of the Cr^{4+} ion in the investigated garnets.

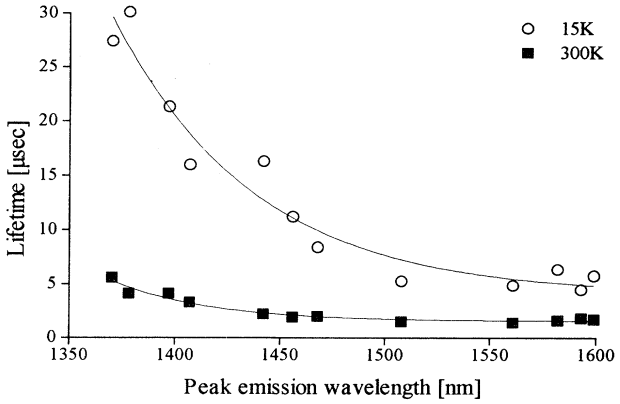

FIG. 4. Lifetime of the Cr^{4+} ion at 15 and 300 K as a function of the peak emission wavelength. The solid curves are just for clarity.

In the case of the Cr^{4+}:YAG this ratio can be determined by a calorimetric measurement. Cr^{4+}:YAG exhibits a strong absorption band between 400 and 550 nm,[14] which neither belong to Cr^{3+} nor to tetrahedral Cr^{4+}, but probably to octahedrally coordinated Cr^{4+}. However, under excitation with the 514.5 nm line of an argon-ion laser, the crystal shows no detectable emission between 500 and 2000 nm. Therefore, a complete nonradiative relaxation can be assumed, which means a complete transformation of the absorbed energy into heat. On the other hand, excitation with 1064 nm radiation is, in general, followed by both radiative and nonradiative decay. Therefore the following equations hold if the same temperature increase ΔT is generated by choosing corresponding absorbed energies at both excitation wavelengths:

$$E_{\text{abs}}(514.5\text{ nm})=Q=C\Delta T\ ,$$

$$E_{\text{abs}}(1064\text{ nm})=Q+E_r=C\Delta T+E_r\ ,$$

with absorbed energy E_{abs}, heat Q, energy of emitted photons E_r, heat capacity of the crystal C, and temperature increase ΔT.

For the same increase of temperature, the energy of the emitted photons is the difference between the absorbed energies at 1064 and 514.5 nm:

$$E_r=E_{\text{abs}}(1064\text{ nm})-E_{\text{abs}}(514.5\text{ nm})\ .$$

Taking into account the quantum defect between absorption and emission, the quantum efficiency for 1064 nm excitation can be calculated:

$$\eta=\frac{n_r}{n_{\text{abs}}}=\frac{\dfrac{E_r}{h\nu_r}}{\dfrac{E_{\text{abs}}(1064\text{ nm})}{h\nu_{\text{abs}}(1064\text{ nm})}}=\left[1-\frac{E_{\text{abs}}(514.5\text{ nm})}{E_{\text{abs}}(1064\text{ nm})}\right]\frac{h\nu_{\text{abs}}(1064\text{ nm})}{h\nu_r}\ .$$

Because of the Gaussian-like broadband emission, $h\nu_r$ was set to the photon energy at the emission band maximum, i.e., $h\nu_r=7258\text{ cm}^{-1}$.

In Fig. 5 the increase of the temperature of the Cr^{4+}:YAG crystal under 514.5 and 1064 nm excitation as a function of the absorbed energy is shown. From the linear interpolation of both curves the quantum efficiency at room temperature is determined:

$$\eta(300\text{ K})\approx 14\%\ .$$

For an estimation of the accuracy of this value, mainly the assumption of complete nonradiative decay under 514.5 nm excitation has to be evaluated. Although no fluorescence was detected, some weak emission could be possible according to residual absorption into the shoulders of the Cr^{4+} or Cr^{3+} absorption bands. This yields directly an increase in the value for the quantum efficiency, so that 14% has to be considered as a lower limit.

B. Temperature dependence of the transition rate and of the quantum efficiency

The total decay rate W of a transition is the sum of the radiative decay rate W_r and the nonradiative decay rate W_{nr}:

$$W=W_r+W_{nr}=\frac{1}{\tau}=\frac{1}{\tau_r}+\frac{1}{\tau_{\text{nr}}}\ . \tag{1}$$

The quantum efficiency η is defined as the ratio between the radiative rate W_r and the total decay rate W:

$$\eta=\frac{W_r}{W}=\frac{\tau}{\tau_r}\ . \tag{2}$$

The temperature dependence of the radiative decay rate can be expressed by a coth law:[11–13]

$$\frac{1}{\tau_r(T)}=R_{\text{vib}}\coth\left[\frac{E_{\text{vib}}}{2kT}\right]\ , \tag{3}$$

where $R_{\text{vib}}=1/\tau_r(0)$ is the radiative decay rate at 0 K, E_{vib} is the energy of the effective non-totally-symmetric

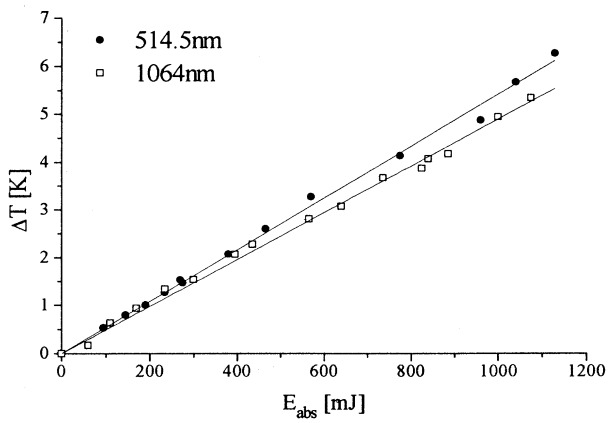

FIG. 5. Temperature increase of the Cr^{4+}:YAG crystal under excitation with a Nd:YAG laser and with an argon-ion laser, respectively. The solid curves are linear fits to the experimental data.

phonon, which couples to the magnetic-dipole transition and induces vibronically electric-dipole transition probability from higher electronic states of opposite parity to the transition, k is the Boltzmann constant, and T is the temperature.

The temperature dependence of the nonradiative rate can be expressed according to the model of Struck and Fonger:[8]

$$W_{\rm nr}=\sum_{m=0}^{\infty}N_{nm}=\sum_{m=0}^{\infty}R_{\rm nr}(1-r_\nu)r_\nu^m\langle u_n|\nu_m\rangle^2\equiv R_{\rm nr}U_p\ , \tag{4}$$

where $R_{\rm nr}$ is the nonradiative decay constant ($\approx 10^{12}-10^{14}$ s^{-1}), $(1-r_\nu)r_\nu^m$ is the thermal occupation of the vibronic level m in the excited electronic state ν ($r_\nu=e^{-\hbar\omega_\nu/kT}$), and $\langle u_n|\nu_m\rangle^2$ is the overlap matrix element between the excited state level ν_m and the ground-state level u_n. For simplification of the model, harmonic potentials and equal force constant ($\hbar\omega_\nu=\hbar\omega_u$) in the ground and in the excited states are assumed. Within the Stirling approximation the total nonradiative rate can be expressed by[9-10]

$$W_{\rm nr}=R_{\rm nr}e^{-S\langle 2m+1\rangle}\frac{e^{p^*}}{\sqrt{2\pi p^*}}\left[\frac{2S\langle 1+m\rangle}{p+p^*}\right]^p \tag{5}$$

with

$$p^*=\sqrt{p^2+4S^2\langle 1+m\rangle\langle m\rangle}\ ,$$
$$\langle m\rangle=\frac{r}{1-r}=\frac{1}{e^{\hbar\omega/kT}-1}\ ,$$

and $r=e^{-\hbar\omega/kT}$. In these equations S is the Huang-Rhys parameter, p is the number of phonons bridging the energy gap between excited state and ground state, and $\omega=\omega_\nu=\omega_u$ is the energy of the effective symmetric phonon. This approximation is valid for $p^*>1$. Therefore $W_{\rm nr}$ at 0 K is given by

$$W_{\rm nr}(0)=R_{\rm nr}\frac{e^{p-S}}{\sqrt{2\pi p}}\left[\frac{S}{p}\right]^p\ . \tag{6}$$

Hence, the nonradiative rate can be expressed in a very convenient form, which is used later for the fit to the experimental data:

$$W_{\rm nr}(T)=W_{\rm nr}(0)\left[\frac{p}{p^*}\right]^{1/2}\left[\frac{2p\langle 1+m\rangle}{p+p^*}\right]^p e^{(p^*-p-2mS)}\ . \tag{7}$$

The total decay rate is given by

$$W=W_r+W_{\rm nr}=W_r(R_{\rm vib},E_{\rm vib})+W_{\rm nr}(R_{\rm nr},\hbar\omega,S,p)$$
$$=R_{\rm vib}\coth\left[\frac{E_{\rm vib}}{2kT}\right]+W_{\rm nr}(0)\left[\frac{p}{p^*}\right]^{1/2}\times\left[\frac{2p\langle 1+m\rangle}{p+p^*}\right]^p e^{(p^*-p-2mS)}\ . \tag{8}$$

Thus the temperature dependence of the decay rate is expressed by six parameters: $R_{\rm vib}$, $E_{\rm vib}$, $R_{\rm nr}$, $\hbar\omega$, S, and p. Before fitting the data with Eq. (8), as much as possible parameters were estimated from independent spectroscopic data. Most of such data are known for Cr^{4+}:YAG, so the discussion starts with this material. Afterwards the temperature dependence of the lifetime of the other investigated Cr^{4+}-doped garnets will be discussed with nearly the same parameters, assuming that the main difference is based on the smaller energy gap between the ground state and the excited state.

The Huang-Rhys parameter S and the phonon energy $E_{\rm vib}$ are estimated from the temperature dependence of the emission bandwidths:[13]

$$\Gamma(T)=\Gamma(0)\left[\coth\left[\frac{E_{\rm vib}}{2kT}\right]\right]^{1/2}$$
$$=2.36\hbar\omega\sqrt{S}\left[\coth\left[\frac{E_{\rm vib}}{2kT}\right]\right]^{1/2}\ . \tag{9}$$

In Fig. 6 the squared emission bandwidths of Cr^{4+}:YAG as a function of temperature are shown. The best fit to the experimental data was achieved with

$$S=2.73\ ,$$
$$E_{\rm vib}=200\ {\rm cm}^{-1}\ .$$

With the quantum efficiency of 14% at 300 K for the emission of the Cr^{4+} ion in YAG—determined from the calorimetric measurement—and the coth law the radiative rate at 0 K is calculated:

$$R_{\rm vib}(0)=\frac{1}{\tau_r(0)}=\frac{\eta(T)}{\tau(T)\coth\left[\frac{E_{\rm vib}}{2kT}\right]}\approx 15\,100\ {\rm s}^{-1}\ .$$

Therefore [see Eq. (1)], $W_{\rm nr}(0)\approx 18\,000$ s^{-1}. Using Eq. (6) with $S=2.73$ and $R_{\rm nr}=10^{14}$ s^{-1}, the number of phonons bridging the energy gap $E_{\rm gap}$ is estimated to be $p\approx 19$ (in comparison, for $R_{\rm nr}=10^{12}$ s^{-1}, p is about 16.5). With $E_{\rm gap}(Cr^{4+}{:}YAG)\approx 7800$ cm^{-1},[15] the energy of the

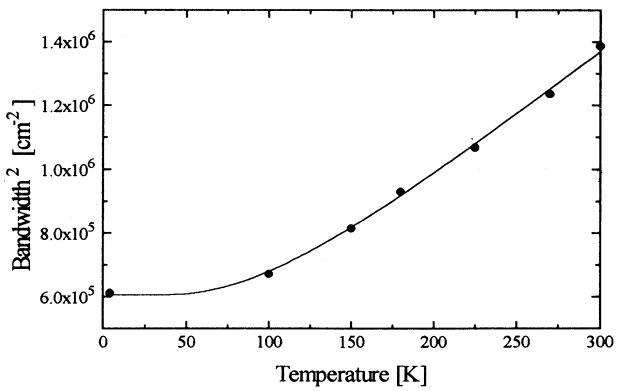

FIG. 6. Squared bandwidth of the Cr^{4+}:YAG emission as a function of the temperature. The solid curve is the best fit to the data using Eq. (9).

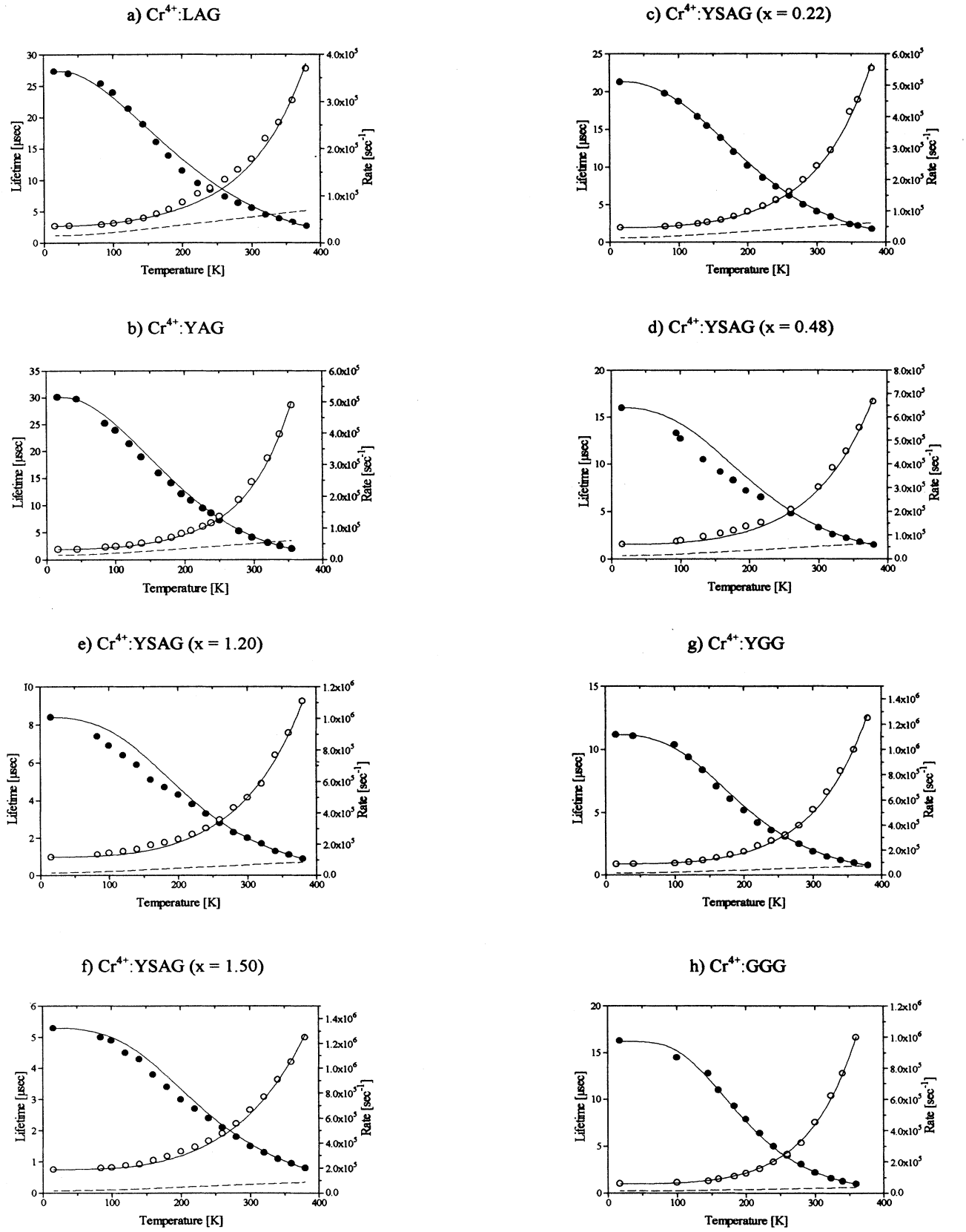

FIG. 7. Temperature dependence of the lifetime (closed circles) and the total emission rate (open circles) for the different garnet crystals. The solid lines are the fitted curves to the experimental data, the dashed line is the radiative rate.

i) Cr^{4+}:YSGG

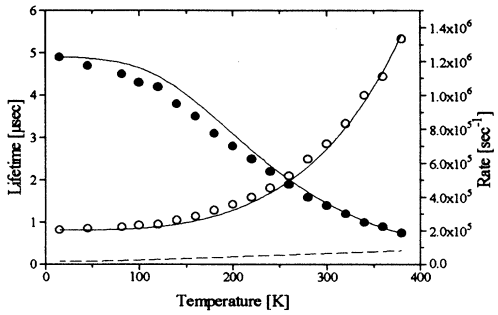

k) Cr^{4+}:GSGG

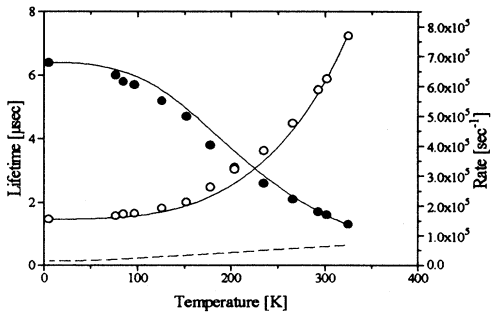

j) Cr^{4+}:GSAG

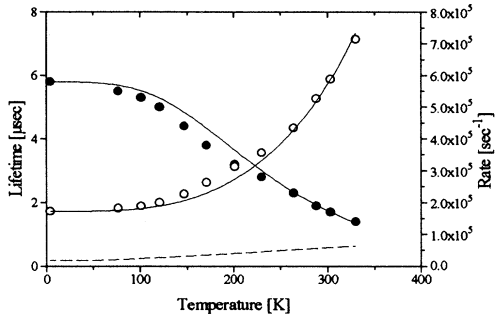

FIG. 7. (*Continued*).

effective phonon for the nonradiative decay is determined:

$$\hbar\omega = \frac{E_{\text{gap}}}{p} \approx 410 \text{ cm}^{-1} .$$

These parameters were used as start parameters in Eq. (8) and only slightly varied. The best fit to the experimental data—see Fig. 7(b)—was achieved with the parameters listed in Table II, which are in reasonable agreement with the spectroscopically determined values.

For the other Cr^{4+}-doped garnet crystals the different energy gaps, i.e., the number of bridging phonons p, were estimated from the shift of the peak emission wavelengths compared to that of Cr^{4+}:YAG. The fits show a good agreement between the model and the experimental data, see Fig. 7(a)–(k), indicating that the above-described model with equal force constants and harmonicity in the ground and excited state is a good approximation for the description of the temperature dependence of the life-

TABLE II. List of the determined fit parameters and the resulting quantum efficiencies at 0 K and at room temperature.

Lattice	$W_{\text{nr}}(0)$ (s^{-1})	$\hbar\omega_{\text{eff}}$ (cm^{-1})	S	p	R_{vib} (s^{-1})	E_{vib} (cm^{-1})	$\eta(0)$ (%)	η (RT) (%)
LAG	19 621	427	2.99	18.4	16 875	132	46	33
YAG	17 802	393	2.88	19.9	15 402	129	46	22
YSAG ($x=0.22$)	31 971	428	2.75	18.0	14 977	130	32	21
YSAG ($x=0.48$)	46 826	431	3.06	17.8	15 674	126	25	18
YSAG ($x=1.20$)	100 301	437	3.03	16.9	18 747	118	16	13
YSAG ($x=1.50$)	168 715	457	2.98	15.7	19 964	122	11	11
YGG	72 147	414	2.96	17.9	17 139	132	19	12
GGG	46 818	395	2.95	19.0	14 532	197	24	8
YSGG	185 259	450	3.04	15.5	18 823	122	9	9
GSAG	153 225	445	3.06	15.3	19 188	141	11	10
GSGG	140 343	435	2.90	15.8	15 907	106	10	10

times. The largest deviations are found for the scandium containing crystals with long emission wavelengths. Probably in these cases the energy gap is too small and the above approximations are no longer valid. The nonradiative relaxation rate, in particular, can be influenced strongly by the anharmonicity of the potential,[16] but this is not considered here. Also the Sc distribution on octahedral and dodecahedral lattice sites may cause deviations.

The calculated quantum efficiencies are shown in Figs. 8(a) and 8(b) as a function of temperature and in Table II the values for 0 and 300 K are listed. At 0 K they are less than unity, indicating that already at low temperatures strong nonradiative decay processes take place. In general, the quantum efficiency is correlated with the energy gap—which is the parameter of large influence—and the corresponding number of bridging phonons p. The Cr^{4+}-doped crystals with the shortest emission wavelengths have the highest quantum efficiencies; for increasing emission wavelengths the quantum efficiency decreases. Also the temperature behavior of the quantum efficiency is nearly the same for all investigated garnet crystals. They show an increase up to 130 K, caused by the coupling of non-totally-symmetric phonons (promoting modes) forcing electric-dipole transition probability. Above 130 K the nonradiative decay processes dominate and the quantum efficiencies decrease. The calculated quantum efficiency of 22% for Cr^{4+}:YAG at room temperature is in satisfactory agreement with the experimental value of 14% from the calorimetric measurement, which was determined as the lower limit.

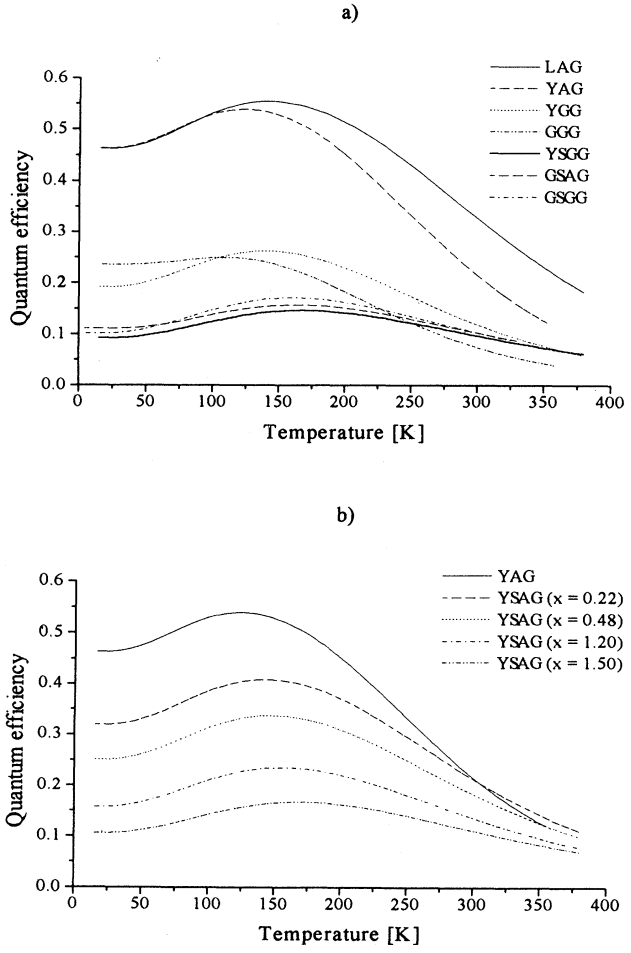

FIG. 8. Temperature dependence of the quantum efficiency of the investigated Cr^{4+}-doped garnet crystals.

C. Emission cross sections

The emission cross section can be determined using the formula of McCumber,[17] which is valid for emissions with a Gaussian bandshape:

$$\sigma_{em}=\eta\left[\frac{\ln 2}{\pi}\right]^{1/2}\frac{1}{4\pi c n^2 \tau}\frac{\lambda^4}{\Delta\lambda}$$

with quantum efficiency η, lifetime τ, refractive index n, peak emission wavelength λ, and emission bandwidth $\Delta\lambda$.

The emission cross sections at room temperature for the investigated crystals are listed in Table I, also. For the characterization of a laser material, the lifetime of the upper laser level and the emission cross section are important parameters, because the laser threshold is proportional to $(\sigma_{em}\tau)^{-1}$. The $\sigma_{em}\tau$- products of the Cr^{4+}-doped garnets are in the order 10^{-24} s cm^2 and therefore comparable to that of Ti^{3+}:Al_2O_3 [$\sigma_{em}\tau=1.4\times10^{-24}$ s cm^2 (Ref. 18)], see Table I. If effects like excited state absorption of the pump or laser wavelength are not considered, it is expected that the best laser results will be obtained with Cr^{4+}:$Lu_3Al_5O_{12}$, Cr^{4+}:$Y_3Al_5O_{12}$, and the Cr^{4+}:$Y_3Sc_xAl_{5-x}O_{12}$ crystals with low scandium content.

V. SUMMARY

In this paper the temperature-dependent lifetime data of the upper laser level of the Cr^{4+} ion in several garnets have been presented and analyzed. At low temperature, they are between 4.9 and 30.1 μs, and at room temperature between 1.3 and 5.6 μs. The decrease of the lifetime is due to the coupling of both symmetric phonons, which raises only the nonradiative decay rate, and non-totally-symmetric phonons, which raises also the radiative decay rate. With these data the quantum efficiency of the Cr^{4+} emission was calculated. It was shown that already at low temperature strong nonradiative relaxations take place, resulting in quantum efficiencies between 9% and 46%. The coupling of non-totally-symmetric phonons yield also an increase in the radiative rate, but above a temperature of 130 K the nonradiative decay processes dominate. Nevertheless, the transition becomes partially electric-dipole allowed due to this coupling. At room temperature, the quantum efficiencies are between 8% and 33%. With a calorimetric method the room-temperature quantum efficiency of Cr^{4+}:YAG could be established experimentally. The emission cross sections are between 3.1×10^{-19} cm^2 and 5.2×10^{-19} cm^2, which are typical values for transition metal ions on tetrahedrally coordinated lattice sites. The $\sigma_{em}\tau$-products are comparable to the value of Ti^{3+}:Al_2O_3.

*Fax: +49-40-4123-6281. Electronic address: KUECK@physnet.uni-hamburg.de

[1]V. Petricevic, S. K.Gayen, R. R. Alfano, K. Yamagishi, H. Anzai, and Y. Yamaguchi, Appl. Phys. Lett. **52**, 1040 (1988).

[2]V. Petricevic, S. K. Gayen, and R. R. Alfano, Appl. Phys. Lett. **53**, 2590 (1988).

[3]H. R. Verdun, L. M. Thomas, D. M. Andrauskas, T. McCollum, and A. Pinto, Appl. Phys. Lett. **53**, 2593 (1988).

[4]A. P. Shkadarevich, *OSA Proceedings on Tunable Solid State Lasers,* edited by M. L. Shand and H. P. Jenssen (Optical Society of America, Washington, D.C., 1989), Vol. 5, pp. 60–65.

[5]G. M. Zverev and A. V. Shestakov, *OSA Proceedings on Tunable Solid State Lasers* (Ref. 4), pp. 66–70.

[6]J. Koetke, S. Kück, K. Petermann, G. Huber, G. Cerullo, M. Danailov, V. Magni, L. F. Qian, and O. Svelto, Opt. Commun. **101**, 195 (1993).

[7]S. Kück, K. Petermann, U. Pohlmann, U. Schönhoff, and G. Huber, Appl. Phys. B **58**, 153 (1994).

[8]C. W. Struck and W. H. Fonger, J. Lumin. **10**, 1 (1975).

[9]H. V. Lauer and F. K. Fong, J. Chem. Phys. **60**, 274 (1974).

[10]W. H. Fonger and C. W. Struck, J. Chem. Phys. **69**, 4171 (1978).

[11]D. S. McClure, Solid State Phys. **9**, 400 (1959).

[12]B. di Bartolo and R. Peccei, Phys. Rev. **137**, A1770 (1965).

[13]B. Henderson and G. F. Imbusch, *Optical Spectroscopy of Inorganic Solids* (Clarendon, Oxford, 1989).

[14]S. Kück, K. Petermann, and G. Huber, *OSA Proceedings on Advanced Solid-State Lasers,* edited by George Dubé and Lloyd Chase (Optical Society of America, Washington, D.C., 1991), Vol. 10, pp. 92–94.

[15]K. R. Hoffman, U. Hömmerich, S. M. Jacobsen, and W. M. Yen, J. Lumin. **52**, 277 (1992).

[16]M. D. Sturge, Phys. Rev. B **8**, 6 (1973).

[17]D. E. McCumber, Phys. Rev. **134**, A299 (1964).

[18]P. Albers, E. Stark, and G. Huber, J. Opt. Soc. Am. B **3**, 134 (1985).

[19]B. Strocka, P. Holst, and W. Tolksdorf, Philips J. Res. **33**, 186 (1978).